J. Am. Soc. Mass Spectrom. (2017) 28:1462–1472
DOI: 10.1007/s13361-017-1650-y

FOCUS: BIO-ION CHEMISTRY: INTERACTIONS OF BIOLOGICAL IONS WITH IONS, MOLECULES, SURFACES, ELECTRONS, AND LIGHT: RESEARCH ARTICLE

SITS Derivatization of Peptides to Enhance 266 nm Ultraviolet Photodissociation (UVPD)

M. Montana Quick,[1] M. Rachel Mehaffey,[1] Robert W. Johns,[2,3] W. Ryan Parker,[1] Jennifer S. Brodbelt[1]

[1]Department of Chemistry, University of Texas, Austin, TX 78712, USA
[2]Department of Chemistry, University of California, Berkeley, CA 94720, USA
[3]McKetta Department of Chemical Engineering, University of Texas, Austin, TX 78712, USA

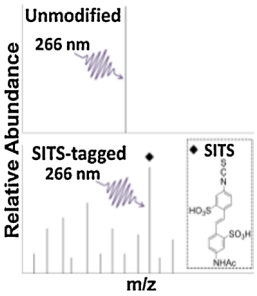

Abstract. N-terminal derivatization of peptides with the chromogenic reagent 4-acetamido-4-isothiocyanatostilbene-2,2-disulfonic acid (SITS) is demonstrated to enhance the efficiency of 266 nm ultraviolet photodissociation (UVPD). Attachment of the chromophore results in a mass shift of 454 Da and provides significant gains in the number and abundances of diagnostic fragment ions upon UVPD. Activation of SITS-tagged peptides with 266 nm UVPD leads to many fragment ions akin to the *a/b/y* ions commonly produced by CID, along with other sequence ions (*c, x,* and *z*) typically accessed through higher energy pathways. Extreme bias towards C-terminal fragment ions is observed upon activation of SITS-tagged peptides using multiple 266 nm laser pulses. Due to the high reaction efficiency of the isothiocyanate coupling to the N-terminus of peptides, we demonstrate the ability to adapt this strategy to a high-throughput LC-MS/MS workflow with 266 nm UVPD.

Keywords: Ion activation, Ultraviolet photodissociation, Derivatization, Peptide

Received: 31 January 2017/Revised: 1 March 2017/Accepted: 3 March 2017/Published Online: 17 March 2017

Introduction

Improvements of established ion activation methods and developments of new ones have advanced the performance metrics of tandem mass spectrometry for numerous proteomics applications, including both bottom-up and top-down strategies [1–6]. Collision-based methods, including low-energy collision induced dissociation (CID) and beam-type higher energy collisional dissociation (HCD), electron-based methods, primarily electron transfer dissociation (ETD), and hybrid activation methods such as electron transfer and higher energy collision dissociation (EThcD) are widely available on many types of mass spectrometers and remain the most popular methods for MS/MS analysis [7–10]. Despite the outstanding versatility and wide adoption of these methods, there are ongoing efforts to develop alternative ion activation methods, such as ones that offer higher energy deposition, ones that afford greater specificity for certain types or classes of molecules, or ones capable of promoting selective bond cleavages. Examples of these include the development of surface induced dissociation [11, 12], charge-transfer dissociation [13, 14], metastable atom-activated dissociation [15, 16], and various photodissociation methods [17–20]. Photodissociation offers several compelling features and opportunities for innovative analytical applications. Depending on the wavelength and flux of photons used for photoactivation, there is a significant ability to vary the energy deposition as has been strategically utilized in recent years for ion spectroscopy applications using tunable lasers [21, 22]. Excitation of peptides and proteins by ultraviolet (UV) photons results in significant energy deposition, which allows access to excited electronic states and provides rich spectra containing *a*, *b*, *c*, *x*, *y*, and *z* type fragments [17, 18, 20, 23, 24]. Using pulsed lasers allows ion activation to be implemented in short activation periods, a feature that has allowed successful implementation of UVPD for high throughput analysis of peptides and proteins [23, 25–27]. Now, even

Electronic supplementary material The online version of this article (doi:10.1007/s13361-017-1650-y) contains supplementary material, which is available to authorized users.

Correspondence to: Jennifer Brodbelt; *e-mail:* jbrodbelt@cm.utexas.edu

light emitting diodes (LEDs) can be used for photodissociation, as reported recently, a development which opens avenues for future low cost implementation of UVPD on many mass spectrometer platforms [28].

Lasers of different wavelengths have been used for photodissociation depending on the objective. For example, 157 and 193 nm UVPD have been utilized for the analysis of peptides and proteins as these macromolecules exhibit significant absorption at these wavelengths [20, 29, 30]. Using other UV or visible wavelengths offers a great degree of selectivity for more specialized applications. As an illustration, disulfide bonds in close proximity to tyrosine and tryptophan residues exhibit preferential cleavage upon 266 nm UVPD [31]. Photoabsorption cross-sections of peptides can be modulated by chemical derivatization to furnish them with suitable chromophores that selectively enhance photodissociation at wavelengths for which the intrinsic photoabsorption cross-sections are low or zero. For instance, while peptides exhibit virtually no absorption at 350 nm, UVPD at this wavelength (i.e., 351 nm using an excimer laser or 355 nm using a tripled Nd:YAG laser) has been utilized in several applications after fixing chromophores to the peptides [32–36]. Chromophore tagging in conjunction with 351 nm UVPD has been used to target cysteine-containing peptides for enhanced characterization of antigen-binding regions of antibodies [32] and to improve de novo sequencing of peptides [33, 34], in addition to other applications [35, 36]. There have also been several reports demonstrating the combination of derivatization and 266 nm UVPD to facilitate the determination of disulfide-bound peptides [37], to elucidate phosphorylation sites of peptides [38, 39], and to empower cysteine-selective proteomics [40], among others [41–43]. An analogous chromophore-attachment concept has been employed to decorate peptides with chromophores in the visible range (473 nm or 532 nm) to enable highly selective MS/MS detection schemes [44, 45]. In addition to providing selectivity in distinguishing classes or types of peptides based on chromophore-mediated UVPD, the metric of selectivity can also be extended to fragment ion classification. For example, the attachment of a chromophore to a specific site, such as exclusively at the N-terminus or C-terminus of a peptide, affords a way to selectively annihilate series of fragment ions that retain the chromophore when exposed to multiple UV laser pulses [33, 34, 46]. This feature provides a way to differentiate with confidence types of fragment ions while also decongesting the resulting fragmentation patterns of peptides.

We have previously reported the use of isothiocyanate chemistry to derivatize the N-termini of peptides to enhance the infrared multiphoton dissociation (IRMPD) efficiency of these peptides through attachment of an IR-chromogenic phosphonate group [47] or to enhance 193 nm UVPD via attachment of aromatic chromophores [48]. Kim et al. reported that derivatization of an aliphatic peptide, ASHLGLAR, with phenyl isothiocyanate significantly decreased the intensity of the laser needed to promote efficient 266 nm photodissociation [49]. The results of these previous studies led us to explore the attachment of UV chromophores via isothiocyanate chemistry for increasing the photodissociation efficiencies of peptides irradiated with 266 nm photons. In the present study, 4-acetamido-4-isothiocyanatostilbene-2,2-disulfonic acid (SITS), an N-terminal derivatization reagent, served as an aromatic chromophore to increase the photoabsorption cross-sections of peptides at 266 nm. This tagging reaction not only greatly increased the photodissociation efficiencies of peptides at 266 nm but also significantly altered the fragmentation patterns compared with 266 nm UVPD of unmodified peptides.

Experimental

Materials and Reagents

Peptides were purchased from American Peptide Company (Sunnyvale, CA, USA). Bovine serum albumin (BSA), equine myoglobin, dithiothreitol (DTT), iodoacetamide, and 4-acetamido-4-isothiocyanatostilbene-2,2-disulfonic acid (SITS) were purchased from Sigma-Aldrich (St. Louis, MO, USA). Mass spectrometry-grade trypsin was obtained from Promega (Madison, WI, USA). LC-MS grade acetonitrile and water were purchased from EMD Millipore (Darmstadt, Germany). Pierce C-18 spin columns used for peptide desalting and LC-MS grade formic acid were obtained from Fisher Scientific (Fair Lawn, NJ, USA).

Digestion, N-Terminal Derivatization, and Sample Preparation

One hundred fifty μg of *E. coli* lysate or 20 μg of BSA or myoglobin were each constituted in 100 μL of 50 mM ammonium bicarbonate buffer (pH 8.5). Disulfide bonds were reduced by adding DTT (250 mM in 50 mM ammonium bicarbonate) to a final concentration of 5 mM in solution and incubating at 55 °C for 30 min. Alkylation of the reduced disulfide bonds was achieved by adding iodoacetamide (500 mM in 50 mM ammonium bicarbonate) to a final concentration of 15 mM and incubating at room temperature in the dark for 30 min. Reduced and alkylated proteins and myoglobin were digested overnight at 37 °C using a 20:1 ratio of lysate to trypsin and a 50:1 ratio of protein to trypsin. All digests were desalted using C-18 spin columns. Individual peptides (10 μL of 1 mM) were derivatized with 100 μL of 10 μg/μL SITS (in 50 mM ammonium bicarbonate, pH 8.5). Tryptic digests of proteins and lysates were derivatized with 300 μL of 10 μg/μL SITS (in 50 mM ammonium bicarbonate, pH 8.5). Samples were reacted in the dark at 55 °C for 3 h or overnight (18–24 hours). Reaction of SITS with the primary amines of N-terminal residues results in a mass shift of 454 Da per peptide.

Mass Spectrometry, Liquid Chromatography, and Photodissociation

All experiments were conducted on a Thermo Scientific Instruments Velos Pro dual-pressure linear ion trap mass spectrometer (San Jose, CA, USA) custom fitted with a Continuum Minilite Nd:YAG laser (San Jose, CA, USA) to

allow UVPD in the high pressure trap. The fourth harmonic of the Nd:YAG was utilized for 266 nm UVPD using approximately 6 mJ per pulse unless otherwise noted (and using an unfocused laser beam). SITS-tagged peptides were introduced by static infusion nanoelectrospray ionization (nanoESI) using a spray voltage of 1.5–2.0 kV and a capillary temperature of 275 °C. SITS-derivatized digests were separated on an Ultimate 3000 RSLCnano liquid chromatography system (Sunnyvale, CA, USA) fitted with a 3.5 cm New Objective Integrafrit trap column (100 µm i.d.) and a 15 cm Picofrit analytical column (100 µm i.d.) (Woburn, MA, USA). Both columns were packed in-house using 3.5 µm X-Bridge C-18 stationary phase. Tryptic digests were constituted in 0.1% formic acid to 250 ng/µL (for individual protein digests) or 1 µg/µL (for *E. coli* digests), respectively, for 1 µL injections. Each injection was preconcentrated on the trap column with 2% acetonitrile and 0.1% formic acid. Mobile phases for separation on the analytical column consisted of 0.1% formic acid in water as eluent A and 0.1% formic acid in acetonitrile as eluent B. A linear gradient from 2% B to 50% B over 50 min (for individual protein digests) or 275 min (for *E. coli* digests) at a flow rate of 300 nL/min was used.

Data-dependent acquisition was performed for all LC-MS/MS methods, in which the MS1 scan was followed by 10 consecutive ion activation events (UVPD or CID) of the most abundant peptide ions. The ion isolation width was 4 *m/z*, and a q_z value of 0.250 was used for CID experiments. For all CID experiments, a normalized collision energy (NCE) of 35% was used during a 10 ms activation time. Due to the pulse repetition frequency (15 Hz) of the 266 nm Nd:YAG laser, only one pulse occurred during a 66 ms interval. As a result, all UVPD experiments using one laser pulse used a 1 ms activation period, and all UVPD experiments using two laser pulses required a 67 ms period. For experiments with more than two laser pulses, each additional pulse required an additional 67 ms of activation time. An ion isolation width of 4 *m/z* and a q_z value of 0.250 were used for UVPD experiments.

Database Searching

All LC-MS/MS data were analyzed using Proteome Discoverer (ver. 1.4.1.14). MS/MS spectra for BSA, myoglobin, and *E. coli* were searched against the reference *Bos taurus* proteome database (UniProtKB), the reference *Equus caballus* proteome database (UniProtKB), or the reference *E. coli* proteome database (UniProtKB), respectively. All searches employed a ±1.0 Da tolerance for precursor ions and a ±0.8 Da tolerance for fragment ions. Oxidation of methionine (+15.995 Da) was included in each search as a dynamic modification. Carbamidomethylation of cysteines (+57.021 Da) and conjugation of N-terminal residues with SITS (453.996 Da) were searched as static modifications. Peptides with fewer than five residues were filtered out and manual verification of database search results was performed.

Results and Discussion

Here we employ isothiocyanate chemistry to append an aromatic chromophore to enhance the absorption of 266 nm photons by peptides. Several criteria were considered when choosing an appropriate chromophore. First, the chromogenic reagent should display high reaction efficiency with peptides. In addition, the reaction should be localized to a specific residue or residues to facilitate computer-automated interpretation of the spectra. Activation of chromophore-tagged peptides by 266 nm photons should promote diagnostic and predictable fragmentation. Finally, the tagging strategy should not degrade the chromatographic properties of the peptides. Several isothiocyanate-type reagents with aromatic chromophores were evaluated with the goal of enhancing 266 nm UVPD, and the SITS tag most completely met the three criteria described above as it showed high reaction efficiency with the primary amine of N-termini and led to CID-like fragmentation of peptides upon 266 nm UVPD. Interestingly, the high absorption efficiency of SITS-tagged peptides when exposed to 266 nm photons was not initially predicted based on the absorbance profiles of the SITS reagent and SITS-modified peptides in solution. The absorbance profiles show relatively modest absorbance at 266 nm (Supplementary Figure S1). Despite the low absorbance in solution, the UVPD efficiency of the SITS-tagged peptide ions in the gas phase was significant.

Another isothiocyanate reagent, 4-sulfophenyl isothiocyanate (SPITC), was also considered. We had utilized SPITC in the past to attach aromatic chromophores to peptides to increase their UVPD efficiencies when exposed to 193 nm photons [48]. SPITC reactions that occur at the N-termini of peptides are reasonably efficient, but two factors made SITS a better option for integration with 266 nm UVPD. First, the photodissociation efficiencies of SITS-tagged peptides were consistently more than 10% greater than the photodissociation efficiencies of SPITC-peptides (based on comparison of the summed fragment ion abundances relative to the abundances of the precursors). Second, the SITS-tagged peptides produced a greater array of diagnostic *b/y* ions upon 266 nm UVPD; some of the analogous fragment ions were missing for the corresponding SPITC-peptides. An example illustrating this outcome is shown in Supplementary Figure S2 for angiotensin I (DRVYIHPFHL), which demonstrates that the b_2, b_3, b_4, y_5, y_6, y_7, and y_8 ions are insignificant or not detected for SPITC-DRVYIHPFHL but are readily identified for the SITS-peptide. Given the better performance of the SITS-tagged peptides upon 266 nm UVPD, the SITS reaction was used for the remainder of the study. (UVPD using 355 nm photons was also briefly examined for the SITS-peptides, but the resulting UVPD fragmentation efficiencies were modest and production of fragment ions was limited, as exemplified by the spectrum in Supplementary Figure S3).

As described below, first the CID and UVPD spectra of a series of model peptides were evaluated to determine the impact of the SITS tag on the fragmentation pathways and dissociation efficiencies. The MS1 spectra were similarly examined

to assess variations in the charge states of the peptides prior to and after the SITS reactions. The changes in fragmentation and distribution of fragment ions upon 266 nm UVPD were evaluated as a function of the number of laser pulses. Finally, tryptic digests of individual proteins (myoglobin, BSA) and proteins from cell lysates were analyzed to provide a greater pool of peptides for evaluating the SITS strategy.

CID and 266 nm UVPD of SITS-Derivatized Peptides

N-terminal derivatization of peptides by the SITS reagent causes a mass shift of 454 Da, as shown in Scheme 1. In some cases, the primary amines on the side-chains of lysines were also observed to undergo SITS-derivatization (data not shown). However, due to the high pKa of the lysine side-chain (~10.5), extensive derivatization of lysines was rarely observed, and thus the SITS modification was restricted to the N-terminus in subsequent database searches. As shown in more detail below, even peptides containing amino acids with aromatic side-chains do not have high photoabsorption cross-sections at 266 nm, and thus the incorporation of the SITS tag transforms weakly absorbing peptides into ones with much higher cross-sections. Supplementary Figure S4 shows the ESI mass spectra of unmodified and SITS-derivatized angiotensin I (DRVYIHPFHL) and highlights the high reaction efficiency of the attachment of a SITS chromophore with basically no residual unreacted peptide left in the solution. In addition to the shift in mass, derivatized peptides display a shift in the charge state distribution biased towards the 2+ charge state compared with the bias toward the 3+ charge state observed for the unmodified peptide. Similar to other sulfonated isothiocyanate reagents used in MS workflows [48], this shift in charge state distribution likely stems from two factors: (1) the acidic sulfonic functional groups of the SITS reagent may be deprotonated and afford at least one negatively charged site per peptide, and (2) the N-terminal primary amine, which is typically favored for protonation of peptides owing to its high basicity, is converted to a significantly less basic dialkylthiourea. This type of behavior echoes that noted by Keough and coworkers in founding studies from two decades ago, where peptides containing a C-terminal arginine were subjected to sulfonic acid derivatization that occurred at the N-terminus [50]. The resulting peptides were determined to be protonated on the C-terminal arginine residue and not the derivatized N-terminus, and post-source decay of these peptides led exclusively to *y*-type ions [50].

A comparison of the CID mass spectra for underivatized and SITS-derivatized angiotensin I (DRVYIHPFHL) is shown in Figure 1. Despite or owing to the size and acidity of the SITS tag, a more extensive array of sequence ions, including three additional *b* ions (b_2, b_3, and b_9), is observed for the SITS-modified peptide compared with the unmodified peptide. The survival of the b_2 ion attests to the fact that the SITS tag is not necessarily deprotonated (otherwise the b_2 product would be neutral). The same type of comparison (MS/MS of unmodified peptide versus SITS-modified peptide) was undertaken using 266 nm UVPD. A dramatic improvement in photodissociation efficiency and sequence coverage is observed for SITS-derivatized angiotensin I compared with the unmodified peptide (Figure 2). This significant degree of enhancement in UVPD efficiency is typical for all other peptides in the present study. In general, activation of SITS-derivatized peptides using 266 nm photons leads to C–N bond cleavage of the peptide backbone, mirroring fragmentation promoted by collisional activation. The dominant formation of conventional *b*/*y* ions and suppressed formation of *c*, *x*, and *z* ions is unusual for 266 nm UVPD [51], and is discussed in more detail later. The complete *b* ion series is produced upon 266 nm UVPD spectra of SITS-derivatized angiotensin I, thus further validating that the acidic sulfonate groups of the tag may remain protonated and therefor does not lead to neutralization of all N-terminal fragment ions.

UVPD of SITS-Derivatized Peptides: Variation of the Number of Laser Pulses

We previously reported that exposing peptides containing N-terminal chromophores to multiple 351 nm laser pulses

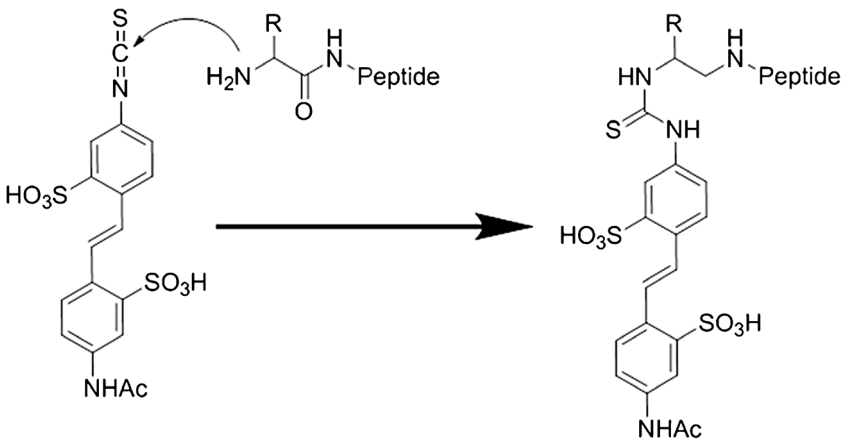

Scheme 1. Derivatization of peptides with the SITS reagent in the presence of ammonium bicarbonate (pH 8.5) results in attachment of a chromophore at the N-terminus (+454 Da mass shift)

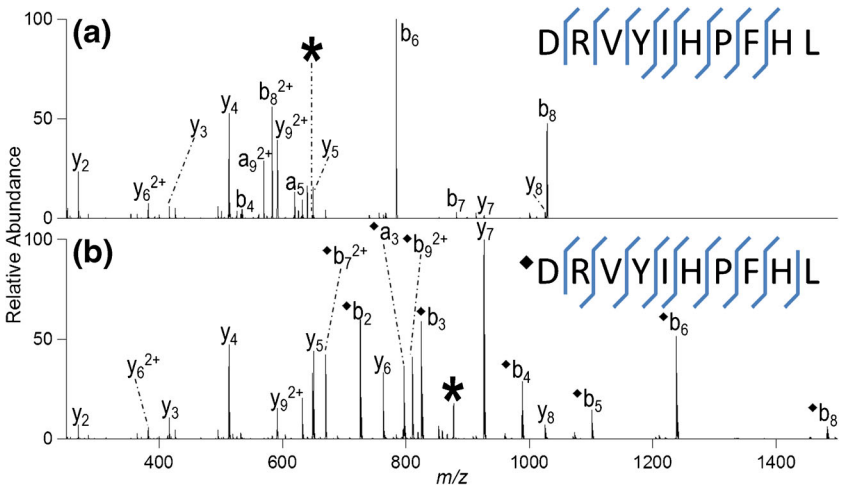

Figure 1. CID mass spectra of **(a)** unmodified angiotensin I (DRVYIHPFHL, 2+), and **(b)** SITS-modified angiotensin I (2+) using NCE of 25%. The precursor ion is labeled with an asterisk. The diamond indicates the presence of the SITS modification

annihilated the N-terminal fragment ions, reducing the complexity of the resulting mass spectra and facilitating de novo sequencing based on spectra that contained clean series of *y* ions [34]. In the present study, SITS-modified peptides were similarly exposed to multiple 266 nm laser pulses to determine the effect of varying pulses on the N-terminal fragmentation of SITS-derivatized peptides. For these experiments, 266 nm UVPD mass spectra were collected in triplicate for unmodified and SITS-tagged angiotensin I while varying the number of pulses. All of the N-terminal *b*-type ions and all of the C-terminal *y*-type ions were summed in order to create the plot shown in Figure 3. The abundances of *y*-type ions always exceed the abundances of *b*-type ions. Moreover, as the number of laser pulses increases, the relative abundance of the N-terminal fragment ions decreases, whereas the relative abundance of C-terminal product ions increases. In contrast, CID of y-type ions generated from the SITS-tagged peptides by UVPD yields MS^3 spectra that contain a mixture of N-terminal and C-terminal (*b* and *y*) fragment ions (Supplementary Figure S5). This collection of results confirms that the SITS-containing *b* ions absorb 266 nm photons and undergo secondary fragmentation (and likely annihilation in many cases) upon exposure to multiple laser pulses; conversely, the chromophore-free *y* ions do not absorb and are unaffected by exposure to additional UV photons.

The distributions of product ions of another peptide, SYSMEHFRWG, upon CID and 266 nm UVPD are displayed in Figure 4 for both the unmodified and SITS-tagged peptide. For this comparison, peptide SYSMEHFRWG was chosen because this peptide contains a sufficient number of aromatic side-chains to allow successful UVPD in the absence of the highly absorbing SITS tag installed at the N-terminus. The fragment ion distributions obtained using five laser pulses for the underivatized and SITS-tagged peptides are strikingly different from each other as well as from the CID results. The relative portions of *a* and *b* ions is significantly lower for the SITS-derivatized peptide; there is an extreme bias towards C-terminal ions. The low prevalence of N-terminal ions, also

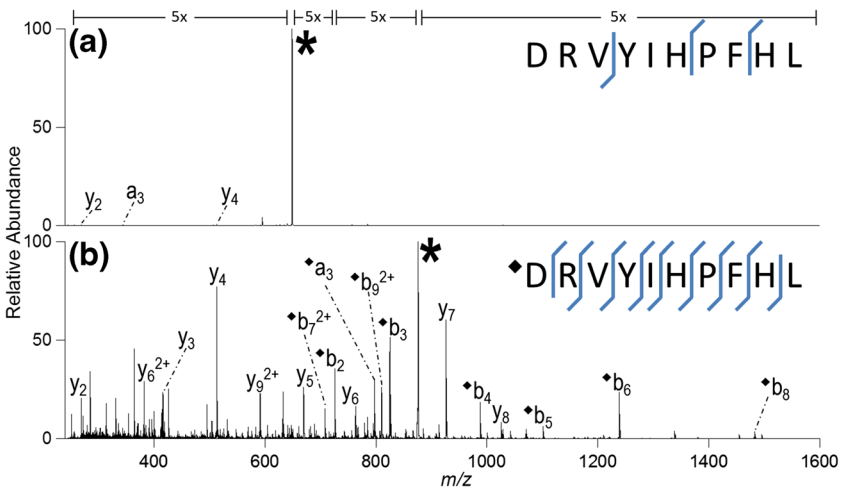

Figure 2. 266 nm UVPD mass spectra of **(a)** unmodified angiotensin I (DRVYIHPFHL, 2+), and **(b)** SITS-modified angiotensin I (2+) using 1 pulse. The precursor ion is labeled with an asterisk. The diamond indicates the presence of the SITS modification. The 5× magnification factors apply to sections of both spectra

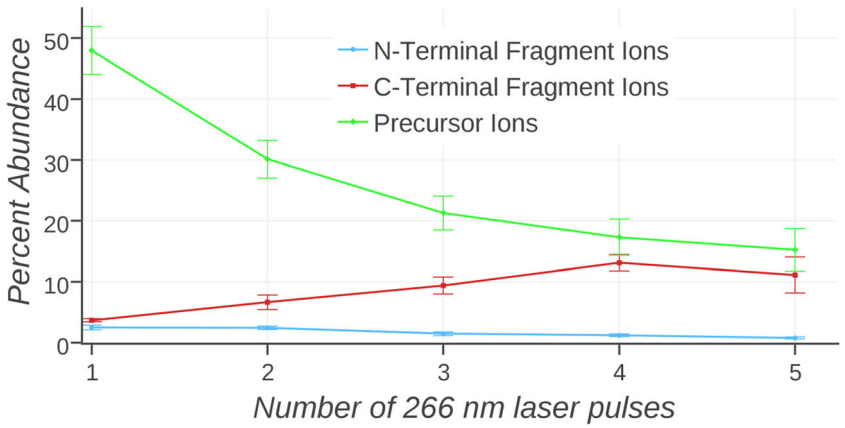

Figure 3. Distribution of N-terminal fragments, C-terminal fragments, and precursor ions as a function of the number of 266 nm laser pulses for angiotensin I (DRVYIHPFHL, 2+)

noted above for angiotensin I, again suggests that the N-terminal ions decompose upon exposure to multiple pulses and thus are converted to nondetectable products. For example, upon 266 nm UVPD, 94% of the products are C-terminal ions for SITS-tagged SYSMEHFRWG compared with just 34% for the unmodified peptide. The distributions of fragment ions upon CID are similar for both the unmodified and SITS-tagged peptide with a more equal distribution of N-terminal *a/b* and C-terminal *y* ions. These results parallel those reported for ESI-MS analysis of N-terminal sulfonic acid derivatized peptides, for which the CID patterns of multiply charged peptides were similar for non-derivatized and sulfonic acid derivatized peptides [52]. These CID and UVPD comparisons are further explored for a greater array of peptides created upon proteolytic digestion of intact proteins in the next section.

SITS Derivatization of Protein and Lysate Digests

Based on the results above, two primary outcomes emerged with respect to the impact of the SITS-derivatization of peptides on 266 nm UVPD. First, addition of the SITS chromophore significantly enhanced the UVPD efficiency owing to the high photoabsorption cross-section of the SITS-tag. Second, the installation of the SITS tag significantly decreased the

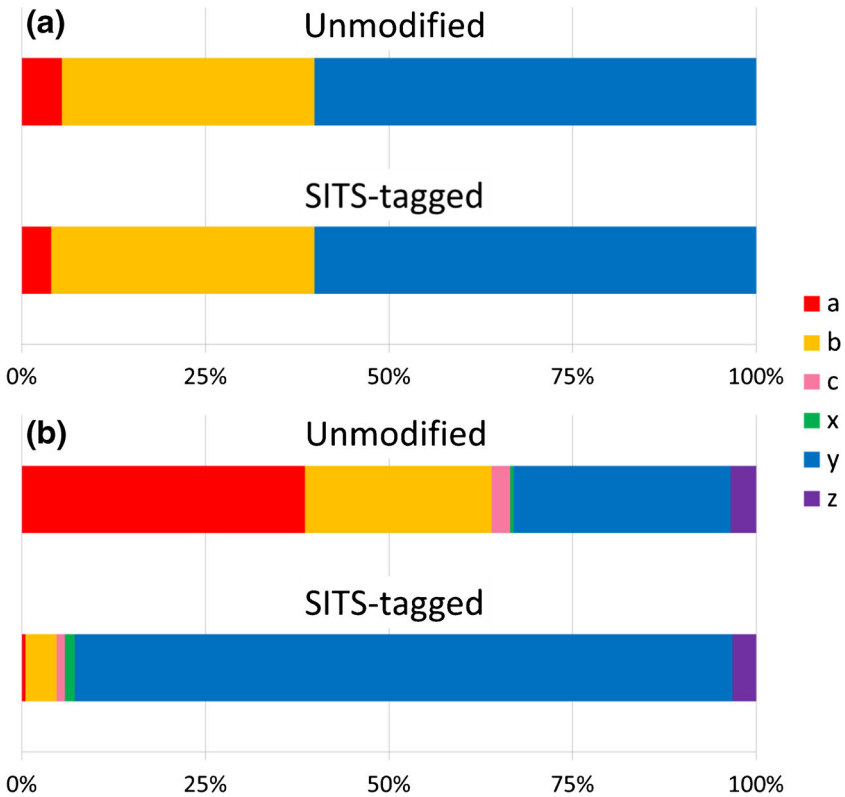

Figure 4. Relative fragment ion distributions of unmodified and SITS-derivatized SYSMEHFRWG (2+) activated by **(a)** CID with an NCE of 20%, or **(b)** UVPD using five laser pulses

relative abundance of N-terminal *a/b* product ions because (1) the high photoabsorption cross-sections of the SITS-tagged fragment ions makes them especially susceptible to UVPD, and (2) neutralization of *a/b* ions owing to the acidic sulfonate moieties of the SITS group. The interesting changes in the fragmentation behavior of SITS-modified peptides noted above were thus examined in greater detail by generating a larger array of SITS-peptides via derivatization of tryptic digests of myoglobin, BSA, or *E.coli* proteins. The general workflow is summarized in Supplementary Scheme S1. Figure 5 shows a pair of base peak chromatograms for the unmodified digest of myoglobin and the corresponding SITS-modified digest, with five of the peptides found in common highlighted. Most of the SITS-tagged peptides were observed predominantly in the 2+ charge state, whereas other corresponding unmodified peptides often displayed a greater distribution of the charge states. The SITS-tagged peptides displayed longer retention times compared with unmodified peptides, presumably owing to the increase in hydrophobicity as a result of the addition of the SITS tag (Figure 5). A comparison of the fragmentation patterns of one representative tryptic peptide (HGTVVLT ALGGILK) from myoglobin is shown in Figure 5c and d. Despite similar sequence coverage, 266 nm UVPD of the SITS-tagged peptide produced the b_2 ion and provided higher relative abundances of several fragment ions compared with CID of the unmodified peptide.

Evaluation of the fragmentation patterns of a greater pool of peptides was undertaken by applying the SITS-derivatization to BSA and *E. coli* tryptic digests. SITS-tagged and unmodified digests were separated via LC, and the eluted peptides were activated in a data-dependent manner by either CID (for the digests containing unmodified peptides or SITS-tagged peptides) or 266 nm UVPD (only for the SITS-tagged peptides). Owing to the low photoabsorption cross-sections of unmodified peptides at 266 nm, very few unmodified tryptic peptides were identified by 266 nm UVPD-MS, and thus the unmodified digests were not analyzed further by UVPD. Direct comparisons of the total number of identified peptides in the BSA digests as well as the number of overlapping peptides identified for each method are summarized in Venn diagrams in Supplementary Figure S6. While CID of the unmodified digest identified more peptides overall, 266 nm UVPD of SITS-tagged BSA digests resulted in identification of a number of unique peptides. For example, while 65 SITS-tagged peptides were identified by UVPD and 96 unmodified peptides were identified by CID, there were 33 that were uniquely found by UVPD. Because the presence of the hydrophobic SITS tag increases the elution times of the peptides, the detection and MS/MS analysis of some peptides that would otherwise co-elute or elute early during a more aqueous part of the gradient are enhanced. This factor accounts for identification of some of the unique SITS-tagged peptides.

Peptides that were successfully identified by three methods: CID (unmodified), CID (SITS-modified), and 266 nm UVPD (SITS-modified), provided the best comparisons for assessing the impact of the SITS tag and the variations caused by collisional activation versus absorption of 266 nm photons. The results for 20 representative peptides from the *E. coli* tryptic digest (all 2+ charge state) are summarized in Figure 6 and Table 1. One set of representative CID/UVPD spectra for *E. coli* tryptic peptide GETQALVTATLGTAR is shown in Supplementary Figure S7. Similar to what was observed in Figure 4, C-terminal ions represent more than 50% of the fragment ion

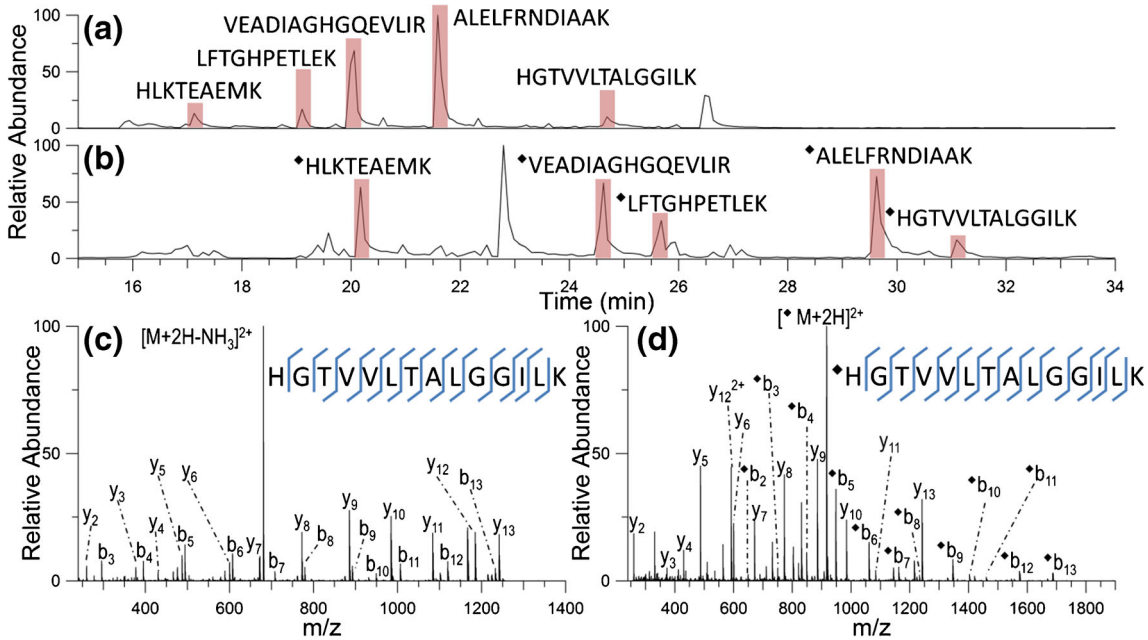

Figure 5. Base peak chromatograms for **(a)** unmodified tryptic digest of myoglobin; **(b)** SITS-modified digest of myoglobin; **(c)** CID spectrum of unmodified tryptic peptide HGTVVLTALGGIK; **(d)** 266 nm UVPD spectrum of SITS-tagged tryptic peptide HGTVVLTALGGIK. A diamond denotes a SITS tag

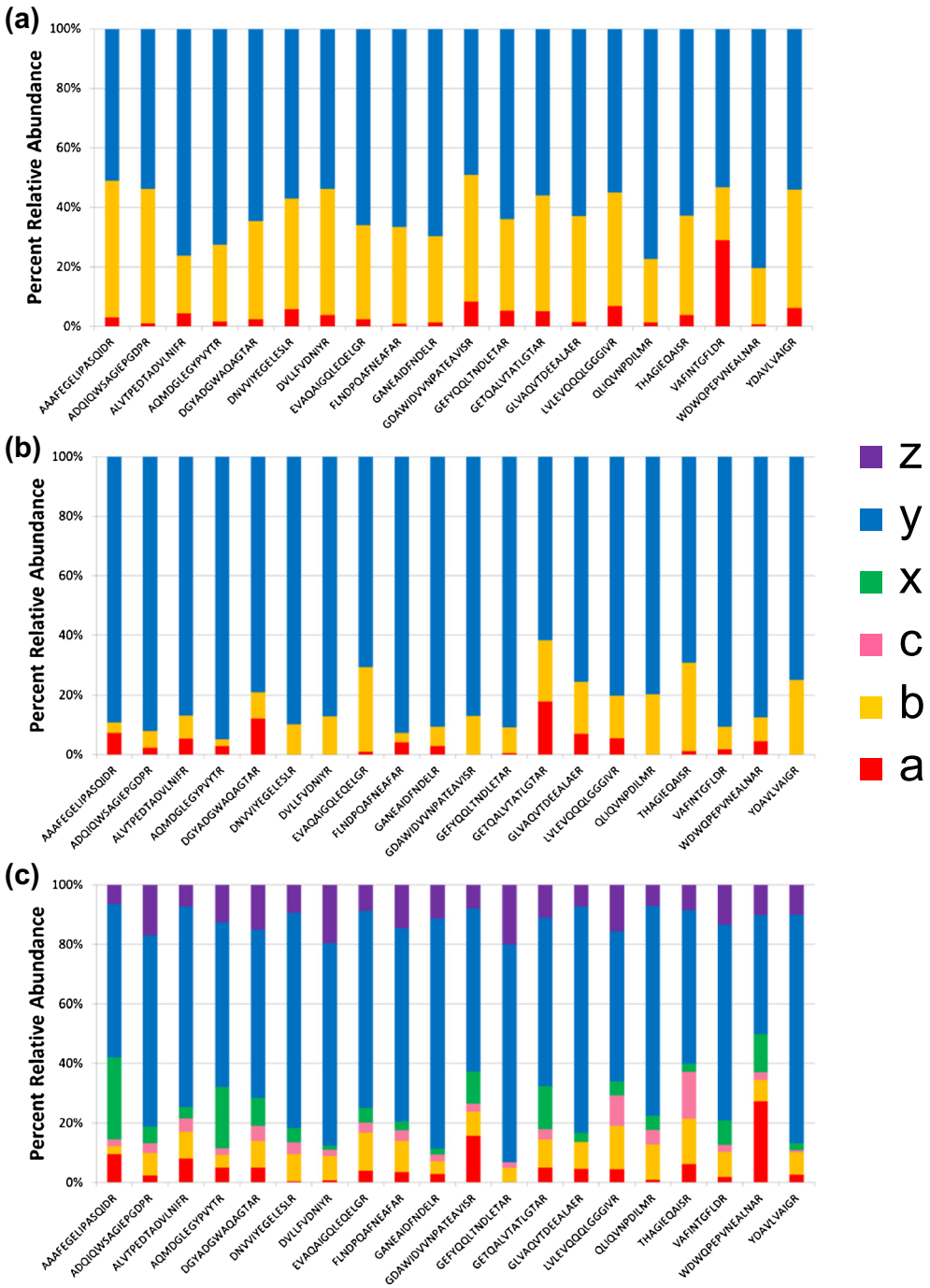

Figure 6. Fragment ion distributions of 20 representative *E. coli* tryptic peptides: **(a)** CID of unmodified peptides, **(b)** CID of SITS-tagged peptides, and **(c)** 266 nm UVPD of SITS-tagged peptides. All peptides are doubly charged (2+). For CID experiments a NCE of 35% was used. For 266 nm UVPD experiments, two 6 mJ pulses was used

distributions of SITS-tagged peptides for both CID and UVPD (Figure 6). The contribution from C-terminal ions (*x*, *y*, *z*) averages 62% for the unmodified peptides (CID data) and increases to 84% and 82% for the SITS-modified peptides activated by CID and UVPD, respectively. UVPD of the SITS-modified peptides produces *x*, *z*, and, in some case, *c* ions that are never observed upon CID, thus underscoring that 266 nm UVPD offers access to some pathways not possible for CID. To decipher the origin of the fragment ions evolving from higher energy pathways (*x*, *z*, *c* ions), a series of experiments were undertaken in which the laser power was attenuated to allow collection of UVPD spectra using nominally 1, 2, 3, 4, 5, or 6 mJ per pulse (for five pulses) (Supplementary Figure S8). As the laser energy increased, the abundance of high-energy fragment ions increased. This result suggests that the higher laser powers enhance the probability for multiphoton absorption, thus contributing to the production of the higher energy fragment ions.

Table 1. Number of *a, b, c, x, y, z* Ions for Unmodified and SITS-Modified Peptides (all 2+) from *E. coli* Tryptic Digest

Peptide	CID unmod a/b/c	CID unmod x/y/z	CID SITS a/b/c	CID SITS x/y/z	UVPD SITS a/b/c	UVPD SITS x/y/z
AAAFEGELIPASQIDR	7	10	6	12	10	28
ADQIQWSAGIEPGDPR	14	11	6	12	4	19
ALVTPEDTADVLNIFR	17	16	16	15	7	24
AQMDGLEGYPVYTR	13	11	4	10	4	15
DGYADGWAQAGTAR	17	14	16	13	6	23
DNVVIYEGELESLR	20	11	8	10	3	17
DVLLFVDNIYR	15	11	11	9	3	11
EVAQAIGQLEQELGR	14	13	6	13	8	18
FLNDPQAFNEAFAR	14	16	12	15	6	14
GANEAIDFNDELR	12	11	12	14	2	18
GDAWIDVVNPATEAVISR	36	19	16	15	4	24
GEFYQQLTNDLETAR	21	14	12	13	3	13
GETQALVTATLGTAR	21	14	21	11	7	24
GLVAQVTDEEALAER	14	15	30	16	3	14
LVLEVQQQLGGGIVR	27	17	13	12	6	12
QLIQVNPDILMR	14	12	5	5	4	11
THAGIEQAISR	12	9	12	13	5	14
VAFINTGFLDR	15	11	2	2	4	9
WDWQPEPVNEALNAR	9	11	7	12	6	14
YDAVLVAIGR	13	8	6	4	2	10

In Table 1, rather than emphasizing the percentage of *a*, *b*, *c*, *x*, *y,* and *z* ions as summarized in Figure 6, the number of *a*, *b*, *c*, *x*, *y*, and *z* sequence ions are tabulated instead. On average, for this set of representative tryptic peptides from the *E. coli* digest, CID yielded 16 N-terminal and 13 C-terminal fragment ions for unmodified peptides, CID yielded 11 N-terminal and 11 C-terminal fragment ions for SITS-modified peptides, and 266 nm UVPD yielded five N-terminal (*a, b, c*) and 17 C-terminal (*x, y, z*) fragment ions for SITS-tagged peptides. The increase in the average number of C-terminal fragment ions for 266 nm UVPD of SITS-tagged peptides over CID of SITS-tagged and unmodified peptides can be attributed to the presence of *x* and *z* fragment ions that result from 266 nm UVPD of chromophore-tagged peptides. Of particular significance is the transformation of the UVPD spectra upon incorporation of the SITS tag: the spectra of the SITS-tagged peptides are consistently rich (Supplementary Figure S7c), akin to the spectra shown in Figure 5d rather than the sparse spectra obtained for underivatized peptides (Figure 2a).

Conclusions

Attachment of the SITS tag to the N-terminus of peptides resulted in significant improvement of 266 nm UVPD, both in terms of the substantial increase in UVPD efficiency and the number of diagnostic sequence ions produced. The SITS reagent exhibited high reaction efficiency with the primary amine of the N-terminus of peptides and led to a more extensive array of fragment ions than obtained using other chromophore-carrying isothiocyanate reagents, like SPITC. The 266 nm UVPD spectra of peptides were transformed from ones that displayed significantly greater portions of *a*, *b*, and *c* ions (for unmodified peptides) to those that were dominated by C-terminal ions (*x*, *y*, *z*) upon incorporation of the SITS tag. Activation of SITS-tagged peptides using 266 nm photons also provided flexibility to produce spectra that contained both N-terminal and C-terminal fragments using one laser pulse to more simplified spectra containing mostly C-terminal fragment ions by employing multiple laser pulses that selectively depleted the chromophore-tagged N-terminal fragment ions. The *c*, *x*, and *z* fragment ions that were produced upon 266 nm UVPD but not generated upon CID of SITS-tagged peptides reflected that higher energy activation pathways were accessible upon activation using 266 nm photons.

Acknowledgements

The authors acknowledge the following funding sources: NSF (Grant CHE1402753) and the Welch Foundation (Grant F-1155). R.W.J. acknowledges an ALS Doctoral Fellowship in Residence and support from the Welch Foundation (F-1848 to Delia Milliron).

References

1. Mayne, J., Ning, Z., Zhang, X., Starr, A.E., Chen, R., Deeke, S., Chiang, C.-K., Xu, B., Wen, M., Cheng, K., Seebun, D., Star, A., Moore, J.I., Figeys, D.: Bottom-up proteomics (2013–2015): keeping up in the era of systems biology. Anal. Chem. **88**, 95–121 (2016)
2. Ahlf, D.R., Thomas, P.M., Kelleher, N.L.: Developing top down proteomics to maximize proteome and sequence coverage from cells and tissues. Curr. Opin. Chem. Biol. **17**, 787–794 (2013)
3. Aebersold, R., Mann, M.: Mass-spectrometric exploration of proteome structure and function. Nature **537**, 347–355 (2016)
4. Gillet, L.C., Leitner, A., Aebersold, R.: Mass spectrometry applied to bottom-up proteomics: entering the high-throughput era for hypothesis testing. Annu. Rev. Anal. Chem. **9**, 449–472 (2016)

5. Toby, T.K., Fornelli, L., Kelleher, N.L.: Progress in top-down proteomics and the analysis of proteoforms. Annu. Rev. Anal. Chem. **9**, 499–519 (2016)
6. Cai, W., Tucholski, T.M., Gregorich, Z.R., Ge, Y.: Top-down proteomics: technology advancements and applications to heart diseases. Expert Rev. Proteom. **13**, 717–730 (2016)
7. Brodbelt, J.S.: Ion activation methods for peptides and proteins. Anal. Chem. **88**, 30–51 (2016)
8. Oh, H.B., Moon, B.: Radical-driven peptide backbone dissociation tandem mass spectrometry. Mass Spectrom. Rev. **34**, 116–132 (2015)
9. Frese, C.K., Altelaar, A.F.M., van den Toorn, H., Nolting, D., Griep-Raming, J., Heck, A.J.R., Mohammed, S.: Toward full peptide sequence coverage by dual fragmentation combining electron-transfer and higher-energy collision dissociation tandem mass spectrometry. Anal. Chem. **84**, 9668–9673 (2012)
10. Qi, Y., Volmer, D.A.: Electron-based fragmentation methods in mass spectrometry: an overview. Mass Spectrom. Rev. **36**, 4-15 (2015).
11. Wysocki, V.H., Joyce, K.E., Jones, C.M., Beardsley, R.L.: Surface-induced dissociation of small molecules, peptides, and noncovalent protein complexes. J. Am. Soc. Mass Spectrom. **19**, 190–208 (2008)
12. Quintyn, R.S., Yan, J., Wysocki, V.H.: Surface-induced dissociation of homotetramers with D2 symmetry yields their assembly pathways and characterizes the effect of ligand binding. Chem. Biol. **22**, 583–592 (2015)
13. Hoffmann, W.D., Jackson, G.P.: Charge transfer dissociation (CTD) mass spectrometry of peptide cations using kiloelectronvolt helium cations. J. Am. Soc. Mass Spectrom. **25**, 1939–1943 (2014)
14. Ropartz, D., Li, P., Fanuel, M., Giuliani, A., Rogniaux, H., Jackson, G.P.: Charge transfer dissociation of complex oligosaccharides: comparison with collision-induced dissociation and extreme ultraviolet dissociative photoionization. J. Am. Soc. Mass Spectrom. **27**, 1614–1619 (2016)
15. Cook, S.L., Zimmermann, C.M., Singer, D., Fedorova, M., Hoffmann, R., Jackson, G.P.: Comparison of CID, ETD, and metastable atom-activated dissociation (MAD) of doubly and triply charged phosphorylated tau peptides. J. Mass Spectrom. **47**, 786–794 (2012)
16. Deimler, R.E., Sander, M., Jackson, G.P.: Radical-induced fragmentation of phospholipid cations using metastable atom-activated dissociation mass spectrometry (MAD-MS). Int. J. Mass Spectrom. **390**, 178–186 (2015)
17. Brodbelt, J.S.: Photodissociation mass spectrometry: new tools for characterization of biological molecules. Chem. Soc. Rev. **43**, 2757–2783 (2014)
18. Reilly, J.P.: Ultraviolet photofragmentation of biomolecular ions. Mass Spectrom. Rev. **28**, 425–447 (2009)
19. Cannon, J.R., Martinez-Fonts, K., Robotham, S.A., Matouschek, A., Brodbelt, J.S.: Top-down 193-nm ultraviolet photodissociation mass spectrometry for simultaneous determination of polyubiquitin chain length and topology. Anal. Chem. **87**, 1812–1820 (2015)
20. Ly, T., Julian, R.R.: Ultraviolet photodissociation: developments towards applications for mass-spectrometry-based proteomics. Angew. Chem. Int. Ed. **48**, 7130–7137 (2009)
21. Cismesia, A.P., Bailey, L.S., Bell, M.R., Tesler, L.F., Polfer, N.C.: Making mass spectrometry see the light: the promises and challenges of cryogenic infrared ion spectroscopy as a bioanalytical technique. J. Am. Soc. Mass Spectrom. **27**, 757–766 (2016)
22. Polfer, N.C.: Infrared multiple photon dissociation spectroscopy of trapped ions. Chem. Soc. Rev. **40**, 2211–2221 (2011)
23. Shaw, J.B., Li, W., Holden, D.D., Zhang, Y., Griep-Raming, J., Fellers, R.T., Early, B.P., Thomas, P.M., Kelleher, N.L., Brodbelt, J.S.: Complete protein characterization using top-down mass spectrometry and ultraviolet photodissociation. J. Am. Chem. Soc. **135**, 12646–12651 (2013)
24. Brodbelt, J.S., Wilson, J.J.: Infrared multiphoton dissociation in quadrupole ion traps. Mass Spectrom. Rev. **28**, 390–424 (2009)
25. Madsen, J.A., Xu, H., Robinson, M.R., Horton, A.P., Shaw, J.B., Giles, D.K., Kaoud, T.S., Dalby, K.N., Trent, M.S., Brodbelt, J.S.: High-throughput database search and large-scale negative polarity LC-MS/MS with ultraviolet photodissociation for complex proteomic samples. Mol. Cell. Proteom. **12**, 2604–2614 (2013).
26. Greer, S.M., Cannon, J.R., Brodbelt, J.S.: Improvement of shotgun proteomics in the negative mode by carbamylation of peptides and ultraviolet photodissociation mass spectrometry. Anal. Chem. **86**, 12285–12290 (2014)
27. Madsen, J.A., Boutz, D.R., Brodbelt, J.S.: Ultrafast ultraviolet photodissociation at 193 nm and its applicability to proteomic workflows. J. Proteome Res. **9**, 4205–4214 (2010)
28. Holden, D.D., Makarov, A., Schwartz, J.C., Sanders, J.D., Zhuk, E., Brodbelt, J.S.: Ultraviolet photodissociation induced by light-emitting diodes in a planar ion trap. Angew. Chem. **128**, 12605–12609 (2016)
29. Cui, W., Thompson, M.S., Reilly, J.P.: Pathways of peptide ion fragmentation induced by vacuum ultraviolet light. J. Am. Soc. Mass Spectrom. **16**, 1384–1398 (2005)
30. Brodbelt, J.S.: Shedding light on the frontier of photodissociation. J. Am. Soc. Mass Spectrom. **22**, 197–206 (2011)
31. Hendricks, N.G., Lareau, N.M., Stow, S.M., McLean, J.A., Julian, R.R.: Bond-specific dissociation following excitation energy transfer for distance constraint determination in the gas phase. J. Am. Chem. Soc. **136**, 13363–13370 (2014)
32. Cotham, V.C., Wine, Y., Brodbelt, J.S.: Selective 351 nm photodissociation of cysteine-containing peptides for discrimination of antigen-binding regions of IgG fragments in bottom-up liquid chromatography-tandem mass spectrometry workflows. Anal. Chem. **85**, 5577–5585 (2013)
33. Robotham, S.A., Kluwe, C., Cannon, J.R., Ellington, A., Brodbelt, J.S.: De novo sequencing of peptides using selective 351 nm ultraviolet photodissociation mass spectrometry. Anal. Chem. **85**, 9832–9838 (2013)
34. Robotham, S.A., Horton, A.P., Cannon, J.R., Cotham, V.C., Marcotte, E.M., Brodbelt, J.S.: UVnovo: a de novo sequencing algorithm using single series of fragment ions via chromophore tagging and 351 nm ultraviolet photodissociation mass spectrometry. Anal. Chem. **88**, 3990–3997 (2016)
35. O'Brien, J.P., Pruet, J.M., Brodbelt, J.S.: Chromogenic chemical probe for protein structural characterization via ultraviolet photodissociation mass spectrometry. Anal. Chem. **85**, 7391–7397 (2013)
36. Aponte, J.R., Vasicek, L., Swaminathan, J., Xu, H., Koag, M.C., Lee, S., Brodbelt, J.S.: Streamlining bottom-up protein identification based on selective ultraviolet photodissociation (UVPD) of chromophore-tagged histidine- and tyrosine-containing peptides. Anal. Chem. **86**, 6237–6244 (2014)
37. Agarwal, A., Diedrich, J.K., Julian, R.R.: Direct elucidation of disulfide bond partners using ultraviolet photodissociation mass spectrometry. Anal. Chem. **83**, 6455–6458 (2011)
38. Diedrich, J.K., Julian, R.R.: Facile identification of phosphorylation sites in peptides by radical directed dissociation. Anal. Chem. **83**, 6818–6826 (2011)
39. Diedrich, J.K., Julian, R.R.: Site-specific radical directed dissociation of peptides at phosphorylated residues. J. Am. Chem. Soc. **130**, 12212–12213 (2008)
40. Parker, W.R., Holden, D.D., Cotham, V.C., Xu, H., Brodbelt, J.S.: Cysteine-selective peptide identification: selenium-based chromophore for selective S–Se bond cleavage with 266 nm ultraviolet photodissociation. Anal. Chem. **88**, 7222–7229 (2016)
41. Parker, W.R., Brodbelt, J.S.: Characterization of the cysteine content in proteins utilizing cysteine selenylation with 266 nm ultraviolet photodissociation (UVPD). J. Am. Soc. Mass Spectrom. **27**, 1344–1350 (2016)
42. Liu, Z., Julian, R.R.: Deciphering the peptide iodination code: influence on subsequent gas-phase radical generation with photodissociation ESI-MS. J. Am. Soc. Mass Spectrom. **20**, 965–971 (2009)
43. Ly, T., Julian, R.R.: Residue-specific radical-directed dissociation of whole proteins in the gas phase. J. Am. Chem. Soc. **130**, 351–358 (2008)
44. Enjalbert, Q., Girod, M., Simon, R., Jeudy, J., Chirot, F., Salvador, A., Antoine, R., Dugourd, P., Lemoine, J.: Improved detection specificity for plasma proteins by targeting cysteine-containing peptides with photo-SRM. Anal. Bioanal. Chem. **405**, 2321–2331 (2013)
45. Enjalbert, Q., Simon, R., Salvador, A., Antoine, R., Redon, S., Ayhan, M.M., Darbour, F., Chambert, S., Bretonnière, Y., Dugourd, P., Lemoine, J.: Photo-SRM: laser-induced dissociation improves detection selectivity of selected reaction monitoring mode. Rapid Commun. Mass Spectrom. **25**, 3375–3381 (2011)
46. Wilson, J.J., Brodbelt, J.S.: MS/MS Simplification by 355 nm ultraviolet photodissociation of chromophore-derivatized peptides in a quadrupole ion trap. Anal. Chem. **79**, 7883–7892 (2007)
47. Vasicek, L.A., Wilson, J.J., Brodbelt, J.S.: Improved infrared multiphoton dissociation of peptides through N-terminal phosphonite derivatization. J. Am. Soc. Mass Spectrom. **20**, 377–384 (2011)
48. Vasicek, L., Brodbelt, J.S.: Enhancement of ultraviolet photodissociation efficiencies through attachment of aromatic chromophores. Anal. Chem. **82**, 9441–9446 (2010)

49. Oh, J.Y., Moon, J.H., Lee, Y.H., Hyung, S.-W., Lee, S.-W., Kim, M.S.: Photodissociation tandem mass spectrometry at 266 nm of an aliphatic peptide derivatized with phenyl isothiocyanate and 4-sulfophenyl isothiocyanate. Rapid Commun. Mass Spectrom. **19**, 1283–1288 (2005)
50. Keough, T., Youngquist, R.S., Lacey, M.P.: Sulfonic acid derivatives for peptide sequencing by MALDI MS. Anal. Chem. **75**, 156A–165A (2003)
51. Robotham, S.A., Brodbelt, J.S.: Comparison of ultraviolet photodissociation and collision induced dissociation of adrenocorticotropic hormone peptides. J. Am. Soc. Mass Spectrom. **26**, 1570–1579 (2015)
52. Bauer, M.D., Sun, Y., Keough, T., Lacey, M.P.: Sequencing of sulfonic acid derivatized peptides by electrospray mass spectrometry. Rapid Commun. Mass Spectrom. **14**, 924–929 (2000)